

Coherent Phonons in Epitaxial Thin Films of Phase-Change Material GeTe

Felix Hoff,* Jonathan Frank, Timo Veslin, and Matthias Wuttig

This study aims to characterize and control coherent phonons in thin GeTe films, a material which has significant potential in advancing optoelectronic technologies. Using femtosecond optical pump-probe spectroscopy, the influence of film thickness, excitation fluence, and excitation polarization on Raman-active phonon modes is investigated. Upon reducing the film thickness from bulk-like to less than 5 nm, the fluence-induced softening of the A_{1g} mode is enhanced by an order of magnitude. In addition, the time-domain measurement of the E_{g} phonon mode in GeTe is reported. By changing the excitation polarization and using double-pulse excitation techniques, these coherent phonons can be enhanced or suppressed as desired. These findings help to develop ultrafast optoelectronic devices and enable novel applications of phase-change materials.

1. Introduction

Germanium telluride (GeTe) has emerged as a promising prototype phase-change material (PCM), having demonstrated remarkable versatility across a variety of applications, including non-volatile memory devices, [1–4] photonic applications, [5,6] and even thermoelectric materials. [7–12] The property portfolio of GeTe makes it an attractive candidate for miniaturized applications, particularly in the realm of electronics where efficient thermal management is crucial. [5,13] To allow for enhanced performance and ensure successful usage in compact devices, thin films of high quality are essential for these applications. [14,15]

A notable characteristic of GeTe is the strong dependence of physical properties on sample thickness. [14,16,17] This

F. Hoff, J. Frank, T. Veslin, M. Wuttig Institute of Physics IA RWTH Aachen University Sommerfeldstraße, 52074 Aachen, Germany E-mail: hoff@physik.rwth-aachen.de

M. Wuttig Peter-Grünberg-Institute JARA-Institute Energy Efficient Information Technology (PGI-10) Wilhelm-Johnen-Straße, 52428 Jülich, Germany

The ORCID identification number(s) for the author(s) of this article can be found under https://doi.org/10.1002/pssr.202500125.

© 2025 The Author(s). physica status solidi (RRL) Rapid Research Letters published by Wiley-VCH GmbH. This is an open access article under the terms of the Creative Commons Attribution License, which permits use, distribution and reproduction in any medium, provided the original work is properly cited.

DOI: 10.1002/pssr.202500125

phenomenon can be attributed to the material's distinct bonding mechanism, known as metavalent bonding,^[14,16] which refers to a situation where, on average, one p-electron is shared between adjacent atoms. [18] This unique electronic configuration describes a competition between electron localization and electron delocalization. This competition leads to significant changes in the atomic arrangement when subjected to variations in film thickness.[19] Our previous results have indicated that both GeTe and bismuth exhibit a sensitive response of their atomic structures to changes in film thickness through what is termed Peierls-like distortion—a structural distortion that lowers symmetry,

changes the film properties and can lead to new electronic phases. $^{[16,20]}$

One property that undergoes substantial alteration under thickness confinement is phonon frequencies. $^{[14,16]}$ These frequencies are intrinsically linked to changes in the bonding mechanism and the resulting alterations in Peierls distortion. $^{[14,16]}$ Under ambient conditions, GeTe crystallizes in a trigonal $R\overline{3}m$ structure, in which two Raman-active phonon modes are typically observed at the zone center: a fully symmetric out-of-plane A_{1g} mode and a lower-symmetric in-plane E_{g} mode. These modes have been investigated through Raman spectroscopy—particularly with respect to the effects of film thickness and pressure $^{[16,21]}$ —but there remains a notable scarcity of time-domain studies examining these phonons. While there are studies of the A_{1g} mode on single crystals, $^{[22,23]}$ there are no measurements of coherent phonons in GeTe thin films and no studies of the E_{g} mode, to our knowledge.

Thus, to investigate this knowledge gap, femtosecond (fs) pump-probe spectroscopy is utilized to investigate the phonon modes in high-quality GeTe thin films at ambient temperature. These films, with thicknesses ranging from 3 to 50 nm, are epitaxially grown on Si(111) substrates using molecular beam epitaxy (MBE).^[16]

The primary objective of this study is to methodically investigate the impact of excitation fluence and polarization on phonon dynamics. The employment of a double-pump excitation approach facilitates the demonstration of enhanced control over phonon modes within these films. This technique enables the manipulation of material properties at ultrafast timescales, a capability that is of great interest for future technological applications. Therefore, this investigation deepens our understanding of how structural and bonding related changes influence phonon behavior at nanoscale dimensions and fs timescales.

2. Results

2.1. Coherent Phonon Softening and Hardening

Transient reflectance in thin GeTe films was recorded using an optical reflection-type fs pump-probe technique to investigate the lattice dynamics. The experimental setup features a two-color fs pump-probe scheme that captures ultrafast changes in transient reflectance for both isotropic and anisotropic (electro-optical) configurations. [24] Measurements were performed in these configurations, enabling the observation of fully symmetric A_{1g} phonon modes (isotropic configuration) and less symmetrical $E_{\rm g}$ phonon modes (anisotropic configuration). [24–26]

Figure 1a shows the isotropic transient reflectance of a 4.6 nm thin sample at an incident pump fluence of 0.58 mJ/cm². The initial change in reflectance, which occurs within the first few hundred fs after photoexcitation, is primarily due to the rapid increase in carrier temperature and the generation of electronhole pairs, which modify the material's dielectric function. [27–29] The subsequent recovery of the reflectance signal indicates a cooling of the electronic system as energy is transferred to the

lattice. [28,29] Concurrently, this rise in electron temperature causes atoms to collectively shift toward a new equilibrium position with reduced distortion. [26] These atoms then oscillate coherently around this equilibrium position via the A_{1g} optical phonon mode, a phenomenon that is reflected in the oscillations present in the measurement signal. [26] The optical response on the given timescale can be characterized by a phenomenological model, which includes the initial excitation, the subsequent energy transfer from the electron system to the lattice, and a damped harmonic oscillator operating at a single frequency. The inset shows the Fourier transform of the oscillating contribution of the measurement signal. The frequency of the oscillator fit is shown as a vertical line and is determined to 3.7 THz. This value is slightly higher than the Raman frequency of the $A_{1\sigma}$ phonon mode of GeTe established in the literature (3.6 THz), [30] but closely matches the pump-probe data reported for a GeTe single crystal (3.7 THz). [22] The estimated dephasing time is about 370 fs. This is remarkably short but consistent with the existing literature, which gives a time of 500 fs. [22] This is supported by the width of the FFT peak, which corresponds to a lifetime broadening of around 440 fs (FWHM).

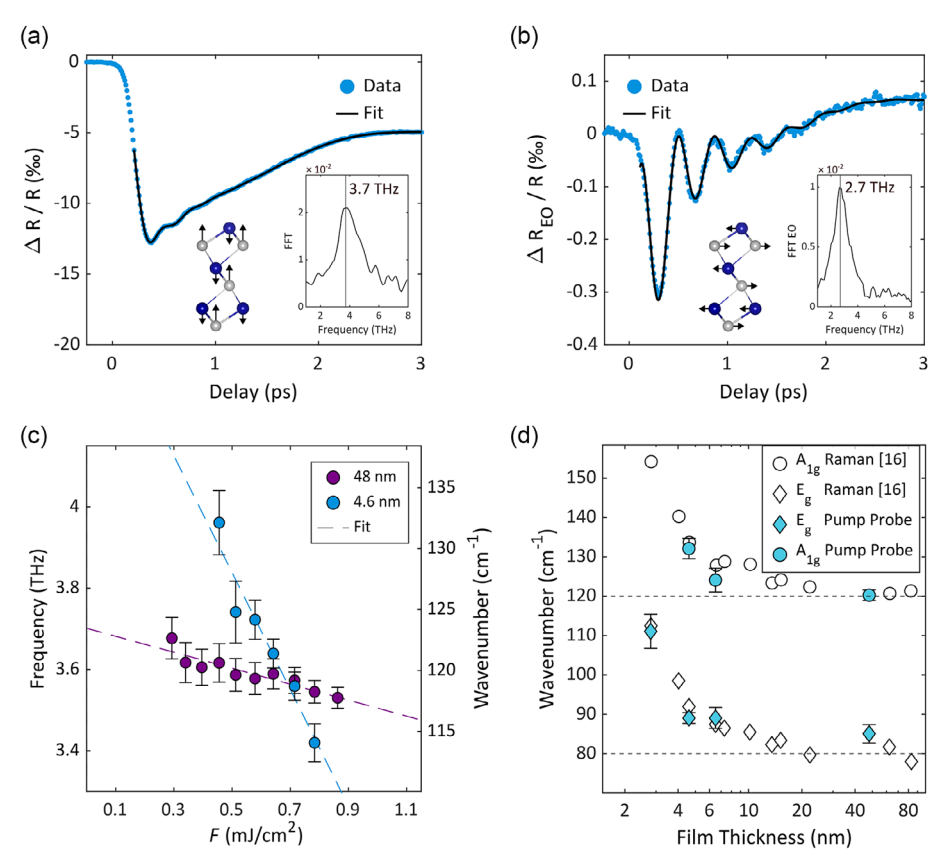


Figure 1. Transient reflectance of the 4.6 nm thick sample at an incident pump fluence of 0.58 mJ/cm^2 . a) Isotropic and b) anisotropic EO measurement signal shows clear coherent phonon oscillations. The measured data is shown as circles, while the fit is shown as a solid black line. The ball and stick models show the view (in-plane direction) of the unit cell with arrows illustrating the vibration pattern. Insets show Fourier transforms of the oscillating part of the signal, solid vertical lines mark the fits frequency. c) The A_{1g} phonon frequencies from time-domain fits as a function of excitation fluence for two film thicknesses. It can be seen that frequencies soften upon increasing fluence for both thicknesses. Yet, this effect is much more pronounced in the thinner film. d) Phonon wave numbers of the A_{1g} and E_g phonon modes for different film thicknesses compared with the Raman data of. Bulk literature values are marked as dashed lines. Pump probe data points are from measurements at the lowest fluence where oscillations were strong enough for evaluation.



www.advancedsciencenews.com



The corresponding anisotropic measurement data, recorded using electro-optical (EO) sampling, is shown in Figure 1b. This data is derived from a differential measurement of s- and p-polarized components of the reflected probe beam. [24] The signal strength is significantly lower than that of the isotropic measurement due to the differential nature of this acquisition method. However, the oscillatory component is better visible. The same fit model as for the isotropic data was used, with the resulting fit shown as a solid black line. The inset shows the FFT of the oscillatory component, with the frequency of the fit marked. The phonon frequency of 2.7 THz corresponds to the $E_{\rm g}$ mode. This measured value is higher than the bulk Raman values of 2.4 THz. [30] The dephasing time is 450 fs, which is longer than the $A_{\rm 1g}$ mode, but still short compared to many other materials that show values well above 1 ps. [25,31] To our knowledge, this mode has never been measured in GeTe in the time-domain.

The frequency of the A_{1g} mode was shown to be very sensitive to the excitation fluence on a GeTe single crystal, [22] with the frequency decreasing significantly with increasing fluence. This effect is called fluence-induced phonon softening and is well known for bismuth. [32–36] To investigate this effect for the thin films in this study, a thick sample (48 nm) and a thin sample (4.6 nm) were measured and analyzed in the incident fluence range between $0.3 \,\mathrm{mJ/cm^2}$ and $0.9 \,\mathrm{mJ/cm^2}$. The A_{1g} mode frequencies for both film thicknesses are shown as a function of fluence in Figure 1c. For both film thicknesses, the phonon frequency reduces with increasing fluence. While the effect is moderate for the thicker sample with a change of 4%, it is much more pronounced for the thin sample, which shows a reduction of 14% between the highest and lowest fluence. In both cases, the trend appears linear, as indicated by the dashed lines representing the linear fit. The increase in the strength of the effect with decreasing film thickness aligns with observations made in thin bismuth films. [20,34] Results for the E_g mode are presented in Figure S1, Supporting Information and exhibit similar behavior but are less pronounced.

Finally, it is remarkable how the frequency of the thinner sample at low fluences deviates from the bulk Raman literature value. This may seem unusual at first, but it fits with the expectations from previous studies, which have already shown a strong increase in both phonon frequencies with decreasing film thickness.^[16,17] In order to verify that this effect can actually be measured in the time-domain, we have examined two additional layers with thicknesses of 2.8 nm and 6.6 nm. For comparability, the samples were measured at the lowest fluence at which the oscillations could be evaluated, see Figure S2, Supporting Information. The resulting phonon frequencies of these measurements are shown in Figure 1d together with the Raman literature values.^[16] It can be seen that the Raman data are in good agreement with the pump-probe data at low excitation fluence. In the 2.8 nm film, the $E_{\rm g}$ mode frequency rises by about 25 cm⁻¹ compared to the thickest film, whereas in the 6.6 nm film, the A_{1g} mode increases by ${\approx}10\,\text{cm}^{-1}$ relative to the thickest film. A similar result has been observed for thin bismuth films. [20] Note that the A_{1g} oscillation amplitude in the thinnest sample is so small that it was not measurable while the E_g mode was observed. The confinement induced phonon hardening seen in these samples is closely related to the chemical bonding in GeTe.[16,18]

2.2. Coherent Phonon Manipulation beyond the Excitation Fluence

In the previous section, two ways of manipulating the frequency of coherent phonons in GeTe thin films were shown. First, by the thickness of the film, which passively controls the phonon dynamics via a change in the intrinsic material properties. The second way is by actively changing the excitation fluence, which has a strong influence on the frequency, amplitude and dephasing time of the coherent phonons. In the following section, we will describe two more approaches to actively manipulate coherent phonons and subsequently, show how they can be used to control the coherent phonons in GeTe.

The vibrational modes that are excited depend on various factors, including the polarization of the pump pulse and the phonon symmetries of the material being studied. This allows for the suppression of specific phonon modes by selecting an appropriate pump pulse polarization, as has been shown for Sb, Bi, and Sb_2Te_3 . [37–39]

Due to the A_{1g} mode being fully symmetric in the out-of-plane direction, the isotropic transient reflectance remains unaffected by the rotation of the pump polarization, as can be seen in Figure S3. This indicates that, at the wavelength used to excite the sample, light absorption in GeTe does not vary with polarization. Since the lower-symmetry E_g mode oscillates in the inplane direction, a change in the anisotropic transient reflection data is expected. Figure 2a shows such data for the 4.6 nm sample. As can be seen, the pump polarization has a significant effect on the phononic response of the material. Figure 2b shows the background subtracted part of the measurement signal for one full rotation of the pump polarization. A clear $\pi/2$ periodicity can be seen in the signal, as indeed expected based on the Raman tensor of the E_g mode in GeTe. To analyze this in more detail, the FFT amplitudes at the E_g mode frequency were determined by peak-fitting for all polarization angles. The result is shown as a polar plot in Figure 2c. The blue solid line shows that the firstorder approximation fits well for the intensity of the E_g mode, which is $I_{E_a} \propto c^2 \cos^2(2\phi)$. A detailed description of the polarization dependence and the Raman tensors can be found in the Supporting Information. These results thus demonstrate that the strength of the E_g phonon mode in thin GeTe films can be controlled and even suppressed significantly with the polarization of the exciting light.

After showing how to control the excitation of the in-plane $E_{\rm g}$ mode with the polarization of the excitation beam, the $A_{\rm 1g}$ mode remains ubiquitous in the material. To control the fully symmetric $A_{\rm 1g}$ mode, a double-pulse excitation can be used. In such an experiment, the inter-pump delay $\Delta \tau$ is defined as the time between the arrival of two consecutive pump pulses. The resulting measurement data of such double-pump excitations and their influence on the transient reflectance are shown in **Figure 3**a using the 48 nm sample. In order to highlight the effect after the arrival of the second pump pulse, the measurement curve before the second pump is shown as faded lines. The modulation of the oscillation amplitude is clear when comparing the top two curves with $\Delta \tau = 100$ fs and $\Delta \tau = 150$ fs. With an inter-pump delay of 150 fs, the oscillation amplitude is noticeably suppressed.

18626270, 2025, 7, Downloaded from https://onlinelibrary.wiley.com/doi/10.1002/pssr.202500125 by Forschungs

zentrum Jülich GmbH Research Center, Wiley Online Library on [30/10/2025]. See the Terms

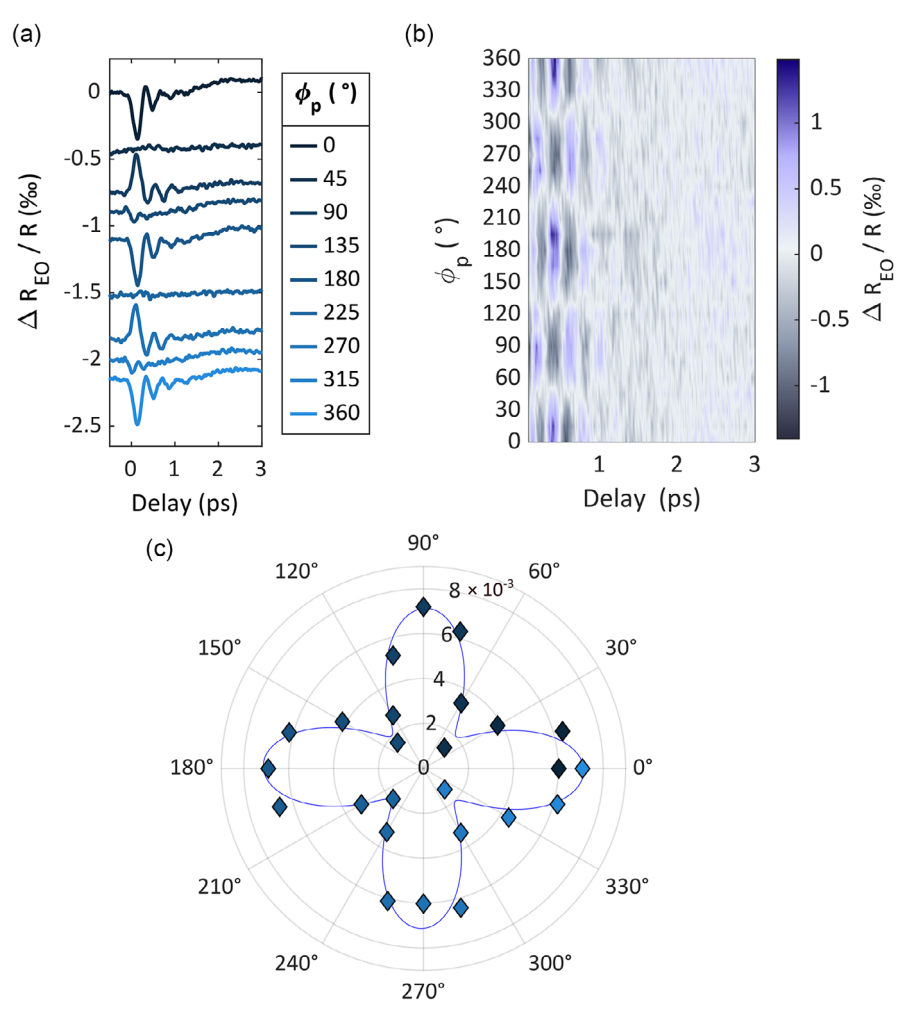


Figure 2. a) Anisotropic transient reflectance for several linear pump polarization angles with an offset for clarity. b) Background-subtracted anisotropic transient reflectance for all polarization angles shows the influence on phononic behavior. c) FFT peak amplitude at the E_g mode frequency presented as a polar plot. The solid line presents the fitted $\cos^2(2\phi)$ dependence leading to the $\pi/2$ periodicity.

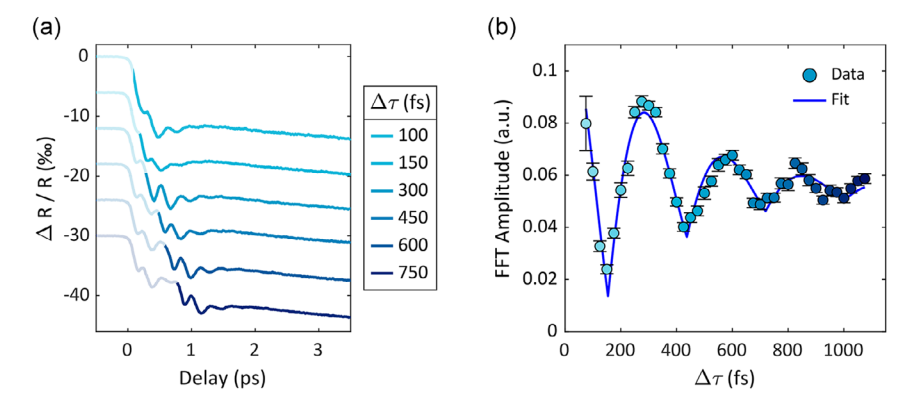


Figure 3. a) Isotropic transient reflectance curves after double-pulse excitation for different inter-pump delays $\Delta \tau$. To focus on the material response after the second pump, the region before the second pump is shown as faded lines. The curves are shifted vertically for clarity. b) Amplitude of the fitted FFT peak as a function of inter-pump delay $\Delta \tau$. The modulation of the amplitude follows a $|\cos(\Delta \tau)|$ behavior and a corresponding fit can be seen as a solid line.

www.advancedsciencenews.com



To test how effectively the second pulse can be used to attenuate or amplify the excited coherent phonons, the oscillatory component of the data after the second pump pulse is analyzed by Fourier transformation. A peak fit provides the associated amplitude as a measure of the oscillation strength. These amplitudes are plotted as a function of the inter-pump delay in Figure 3b. The solid line represents a fitted $|\cos(\Delta \tau)|$ dependence with damping. It can be seen that the modulation of the oscillation amplitude is most effective within the first oscillation period. While the amplitude is strongly suppressed at an inter-pump delay of 150 fs, it is significantly enhanced at 300 fs. At higher inter-pump delays $\Delta \tau$, the modulation efficiency decreases significantly. This is clearly related to the short dephasing time of coherent phonons in GeTe reported in the first part of this study and in the literature.^[22] Thus, it can be seen that double-pulse excitation can be used to amplify and attenuate the coherent A_{1g} phonons in GeTe. However, this only works efficiently within the first period. Moreover, even within this time frame, the rapid decline in the initial amplitude hinders the attainment of complete destructive interference, assuming that both pump pulses have the same fluence. Quantitatively, the transient reflectance amplitude decays to 1/e of its initial value within the first 500 fs after excitation, making efficient interference by applying a second pulse highly unlikely.

3. Discussion and Conclusion

In this study, coherent phonons in GeTe thin films are experimentally investigated using fs laser excitation. Utilizing an isotropic and anisotropic measurement scheme, the low-symmetric $E_{\rm g}$ mode is studied in the time-domain in addition to the fully symmetric $A_{\rm 1g}$ mode. Furthermore, active and passive methods were presented to manipulate the lattice dynamics in GeTe.

The softening of the A_{1g} phonon mode with increasing fluence has already been presented for a single crystal. [22] There, a rate of change of $3.3\,\mathrm{cm}^{-1}/(\mathrm{mJ/cm}^2)$ is found in the linear range of this effect. [22] For the thickest film in this study (48 nm), a more pronounced rate of change of about $8.3\,\mathrm{cm}^{-1}/(\mathrm{mJ/cm}^2)$ can be determined. The transition to the ultrathin film region changes the strength of the effect enormously, as we can determine a rate of change of $50\,\mathrm{cm}^{-1}/(\mathrm{mJ/cm}^2)$ for the $4.6\,\mathrm{nm}$ thick sample. This behavior is consistent with similar studies on isostructural Bi thin films. [34] The increased softening of the A_{1g} mode frequency with excitation intensity toward thin films is attributed to the higher density of excited carriers present in thin films. [34]

Another layer thickness effect that has been studied in both Bi and GeTe is the hardening of the phonon modes toward ultrathin layers. This is closely related to the chemical bonding in these materials and can therefore also be referred to as bond confinement. [14,20] Both materials exhibit metavalent bonding. [20,40] As thickness decreases, bonding changes lead to increased Peierls distortion and unit cell volume, characteristic of metavalent bonding where electron localization competes with delocalization, as can be seen in the room-temperature conductivity. [14,41] Depending on the film thickness, these factors adjust to reach new energy minima by altering atomic positions, a behavior well-documented in thin GeTe layers. [42] This is linked to

cohesive energy per atom and is not strain-related; the effects exceed those from surface or interface influences alone. [43] The bond confinement alters optical and vibrational properties due to reduced interlayer coupling and out-of-plane expansion of the unit cell. While crystal symmetry remains unchanged, this expansion increases the distortion motif and enhances in-plane coupling strength, leading to higher phonon mode frequencies in both in-plane and out-of-plane directions. [14,16,20] As can be seen in Figure 1d, this behavior is confirmed here with time-domain measurements.

Furthermore, the results of this study show that coherent phonons in GeTe thin films can be manipulated by adjusting the polarization of a single fs pump pulse or using two consecutive fs pump pulses. The fully symmetric A_{1g} mode, linked to out-of-plane displacements, remains stable across all polarization angles. In contrast, the in-plane E_{g} mode is highly sensitive to pump polarization, allowing complete suppression or enhancement by changing the polarization angle of the excitation pulse. In addition, a dual-pulse excitation provides further control; by varying the inter-pump delay between pulses, interference effects can be exploited to enhance or reduce the A_{1g} phonon oscillations. While this coherent control is much more effectively utilized in materials with longer dephasing times (like Bi or Sb₂Te₃), it has been shown that it is also possible in GeTe.

The integration of coherent control techniques with coherent phonons enables precise manipulation of light–matter interactions on ultrafast timescales, allowing for enhanced control over phenomena such as electron dynamics and energy transfer. This advancement has significant implications for the development of next-generation optoelectronic devices, improved thermoelectric materials, and the ultrafast tuning of topological properties in quantum systems.

4. Experimental Section

Ultrafast optical measurements were conducted using a standard reflection-type, two-color pump-probe experiment in both isotropic and anisotropic (electro-optic sampling) configurations. The 800 nm wavelength, 60 fs width pump beam was separated from a Ti:Sapphire regenerative fs amplifier, chopped at 1500 Hz, and directed to a free-standing optical delay line before being focused on the sample to a spot size of $300\,\mu m$ in diameter. The probe pulses were frequency converted to 516 nm via sum frequency generation in an optical parametric amplifier and focused to a 30 μm diameter spot on the sample. The determination of spot size and fluence was conducted in accordance with the methodology outlined by Liu. [44] The detection unit comprised two balanced Si photodiodes connected to variable gain current amplifiers and a data acquisition card. To eliminate systematic errors on laboratory time scales, the order of data point recording and the positioning of the delay line were randomized. The anisotropic transient reflectance was calculated from the s- and p-polarized components of the reflected light using the electrooptic detection scheme: $\Delta R_{EO} = \frac{\Delta (R_s - R_p)}{R_0}$, while the isotropic transient reflectance was calculated from the whole signal: $\Delta R = \frac{\Delta(R_s + R_p)}{D}.$ A polarizing beam splitter cube was used to split the reflected probe beam correspondingly. Both, isotropic and anisotropic transient reflectance was normalized to the steady state reflectance R_0 . Reversibility of optical excitation was ensured by monitoring the static reflectance gained for the probe-pulse when the pump-pulse was chopped. By incorporating a rotatable half-wave plate in the pump beam path, the polarization angle Φ_p of the pump pulse relative to the crystal axes of the GeTe thin film can be adjusted. For double-pulse excitation the original pump beam is split and delayed by two delay lines.

The deposition of GeTe thin films was accomplished by means of molecular beam epitaxy (MBE) on a $3.5\times3.5\,\text{cm}^2$ single-side polished Si(111) substrate (N/Ph doped, 3–10 k Ω cm resistivity). The substrate was elevated to a temperature of 750 °C for a duration of 30 min, with the objective of achieving a 7×7 surface reconstruction of Si(111). Without breaking the vacuum, the GeTe films were immediately covered with Al_2O_3 in a dedicated oxide-MBE system. For further information on the sample growth, please refer to the work of Kerres et al. $^{[16]}$

Supporting Information

Supporting Information is available from the Wiley Online Library or from the author

Acknowledgements

F. Hoff, T. Veslin, and M. Wuttig acknowledge financial support from NeuroSys as part of the initiative "Clusters4Future", which is funded by the Federal Ministry of Education and Research BMBF (03ZU2106BA). The authors thank H. Vaishnav and P. Kerres for preparing and characterizing the samples in a previous study. [16] F. Hoff thanks C.F. Schön for invaluable discussions. F. Hoff thanks A. Kiehn for linguistic editing.

Open Access funding enabled and organized by Projekt DEAL.

Conflict of Interest

The authors declare no conflict of interest.

Data Availability Statement

The data that support the findings of this study are available from the corresponding author upon reasonable request.

Keywords

coherent control, coherent phonons, confinement, metavalent bonding, phase-change materials

Received: March 28, 2025 Revised: April 22, 2025 Published online: May 14, 2025

- [1] P. Nukala, C.-C. Lin, R. Composto, R. Agarwal, *Nat. Commun.* 2016, 7, 10482.
- [2] F. M. Schenk, T. Zellweger, D. Kumaar, ACS Nano. 2023, 18. 1063.
- [3] S. Wintersteller, O. Yarema, D. Kumaar, F. M. Schenk, O. V. Safonova, P. M. Abdala, V. Wood, M. Yarema, *Nat. Commun.* 2024, 15, 1011.
- [4] M. Wuttig, N. Yamada, Nat. Mater. 2007, 6, 824.
- [5] A.-K. U. Michel, M. Sousa, M. Yarema, O. Yarema, V. Ovuka, N. Lassaline, V. Wood, D. J. Norris, ACS Appl. Nano Mater. 2020, 3, 4314.
- [6] A. Heßler, I. Bente, M. Wuttig, T. Taubner, Adv. Opt. Mater. 2021, 9, 2101118
- [7] C. Zhang, G. Yan, Y. Wang, X. Wu, L. Hu, F. Liu, W. Ao, O. Cojocaru-Mirédin, M. Wuttig, G. J. Snyder, Y. Yu, Adv. Energy Mater. 2023, 13, 2203361.

- [8] M. Hong, M. Li, Y. Wang, X. L. Shi, Z. G. Chen, Adv. Mater. 2023, 35, 2208272.
- [9] Y. Jiang, B. Su, J. Yu, Z. Han, H. Hu, H.-L. Zhuang, H. Li, J. Dong, J.-W. Li, C. Wang, Nat. Commun. 2024, 15, 5915.
- [10] M. Liu, M. Guo, H. Lyu, Y. Lai, Y. Zhu, F. Guo, Y. Yang, K. Yu, X. Dong, Z. Liu, Nat. Commun. 2024, 15, 8286.
- [11] M. Liu, M. Guo, Y. Yang, X. Dong, H. Lyu, Y. Lai, Y. Zhang, Y. Zhu, H. Wu, F. Guo, Tailoring The Electron And Phonon Transport In Metavalently Bonded GeTe By Stepwise Doping, Advanced Energy Materials, Weinheim, Germany 2025, p. 2405178.
- [12] Y. Yu, X. Xu, M. Bosman, K. Nielsch, J. He, Nat. Rev. Electr. Eng. 2024, 1, 109.
- [13] M. Wang, F. Lin, M. Rais-Zadeh, IEEE Microwave Mag. 2016, 17, 70.
- [14] P. Kerres, R. Mazzarello, O. Cojocaru-Mirédin, M. Wuttig, Phys. Status. Solidi a 2024 221, 2300921.
- [15] P. Mahanta, M. Munna, Technologies 2018, 6, 48.
- [16] P. Kerres, Y. Zhou, H. Vaishnav, M. Raghuwanshi, J. Wang, M. Häser, M. Pohlmann, Y. Cheng, C. F. Schön, T. Jansen, Small 2022, 18, 2201753.
- [17] R. Wang, D. Campi, M. Bernasconi, J. Momand, B. J. Kooi, M. A. Verheijen, M. Wuttig, R. Calarco, Sci. Rep. 2016, 6, 32895.
- [18] M. Wuttig, C. F. Schön, J. Lötfering, P. Golub, C. Gatti, J. Y. Raty, Adv. Mater. 2023, 35, 2208485.
- [19] B. J. Kooi, M. Wuttig, Adv. Mater. 2020, 32, 1908302.
- [20] F. Hoff, P. Kerres, T. Veslin, A. R. Jalil, T. Schmidt, S. Ritarossi, J. Köttgen, L. Bothe, J. Frank, C. F. Schön, Adv. Mater. 2024, 37, 2416938.
- [21] A. Pawbake, C. Bellin, L. Paulatto, K. Béneut, J. Biscaras, C. Narayana, D. J. Late, A. Shukla, Phys. Rev. Lett. 2019, 122, 145701.
- [22] M. Hase, K. Mizoguchi, J. Lumin. 2000, 87, 836.
- [23] M. Hase, M. Kitajima, Appl Phys. Lett 2003, 83, 4921.
- [24] T. Dekorsy, T. Pfeifer, W. Kütt, H. Kurz, Phys. Rev. B 1993, 47, 3842.
- [25] T. Cheng, J. Vidal, H. Zeiger, G. Dresselhaus, M. Dresselhaus, E. Ippen, Appl. Phys. Lett. 1991, 59, 1923.
- [26] H. Zeiger, J. Vidal, T. Cheng, E. Ippen, G. Dresselhaus, M. Dresselhaus, Phys. Rev. B 1992, 45, 768.
- [27] A. Othonos, J. Appl. Phys. 1998, 83, 1789.
- [28] T. Shin, S. W. Teitelbaum, J. Wolfson, M. Kandyla, K. A. Nelson, J. Chem. Phys. 2015, 143, 194705.
- [29] E. Carpene, Phys. Rev. B: Cond. Matter Mater. Phys. 2006, 74, 024301.
- [30] E. Steigmeier, G. Harbeke, Solid State Commun. 1970, 8, 1275.
- [31] J. Mertens, P. Kerres, Y. Xu, M. Raghuwanshi, D. Kim, C. F. Schön, J. Frank, F. Hoff, Y. Zhou, R. Mazzarello, Adv. Funct. Mater. 2024, 34, 2307681.
- [32] M. DeCamp, D. Reis, P. Bucksbaum, R. Merlin, Phys. Rev. B 2001, 64, 092301.
- [33] T. Shin, J. W. Wolfson, S. W. Teitelbaum, M. Kandyla, K. A. Nelson, Phys. Rev. B 2015, 92, 184302.
- [34] F. Thiemann, G. Sciaini, A. Kassen, U. Hagemann, Phys. Rev. B 2022, 106, 014315.
- [35] K. Sokolowski-Tinten, R. Li, A. H. Reid, S. P. Weathersby, F. Quirin, T. Chase, R. Coffee, J. Corbett, A. Fry, N. Hartmann, New J. Phys. 2015, 17, 113047.
- [36] S. L. Johnson, P. Beaud, E. Vorobeva, C. J. Milne, É.D. Murray, S. Fahy, G. Ingold, *Phys. Rev. Lett.* **2009**, *102*, 175503.
- [37] K. Ishioka, M. Kitajima, O. V. Misochko, J. Appl. Phys. 2006, 100, 093501.
- [38] K. Ishioka, M. Kitajima, O. V. Misochko, J. Appl. Phys. 2008, 103, 123505.

on Wiley Online Library for rules of use; OA articles are governed by the applicable Creative Commons



www.advancedsciencenews.com



- [39] K. Norimatsu, M. Hada, S. Yamamoto, T. Sasagawa, M. Kitajima, Y. Kayanuma, K. G. Nakamura, J. Appl. Phys. 2015, 117, 143102.
- [40] O. Cojocaru-Mirédin, Y. Yu, J. Köttgen, T. Ghosh, C. F. Schön, S. Han, C. Zhou, M. Zhu, M. Wuttig, Adv. Mater. 2024, 36, 2403046.
- [41] J. Yanez-Limon, J. González-Hernández, J. Alvarado-Gil, I. Delgadillo, H. Vargas, Phys. Rev. B 1995, 52, 16321.
- [42] R. Wang, W. Zhang, J. Momand, I. Ronneberger, J. E. Boschker, R. Mazzarello, B. J. Kooi, H. Riechert, M. Wuttig, R. Calarco, NPG Asia Mater. 2017, 9, e396.
- [43] I. Ronneberger, Z. Zanolli, M. Wuttig, R. Mazzarello, Adv. Mater. 2020, 32, 2001033.
- [44] J.-M. Liu, Opt. Lett. 1982, 7, 196.